NASA TECHNICAL NOTE

NASA TN D-6380
C.1

TECH LIBRARY KAFB, NM
0132895

LOAN COPY: RETURN
AFWL (DOGL)
KIRTLAND AFB, N. M.

NASA TN D-6380

SUPERCONDUCTING PROPERTIES OF NIOBIUM FILMS

by Wayne R. Hudson and Russell J. Jirberg

Lewis Research Center
Cleveland, Ohio 44135

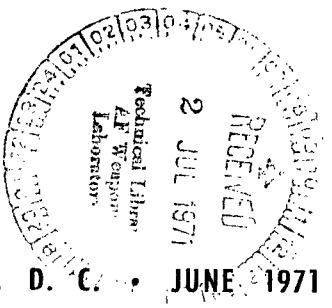

NATIONAL AERONAUTICS AND SPACE ADMINISTRATION • WASHINGTON, D. C. • JUNE 1971

TECH LIBRARY KAFB, NM
0132895

1. Report No.	2. Government Accession No.	3. Recipient's Catalog No.
NASA TN D-6380		

4. Title and Subtitle
SUPERCONDUCTING PROPERTIES OF NIOBIUM FILMS

5. Report Date
June 1971

6. Performing Organization Code

7. Author(s)
Wayne R. Hudson and Russell J. Jirberg

8. Performing Organization Report No.
E-6206

9. Performing Organization Name and Address
Lewis Research Center
National Aeronautics and Space Administration
Cleveland, Ohio 44135

10. Work Unit No.
129-02

11. Contract or Grant No.

12. Sponsoring Agency Name and Address
National Aeronautics and Space Administration
Washington, D. C. 20546

13. Type of Report and Period Covered
Technical Note

14. Sponsoring Agency Code

15. Supplementary Notes

16. Abstract

Critical currents as a function of magnetic field, film thickness, and film orientation have been studied for 14 niobium films ranging in thickness from 16.2 to 1153 nanometers (162 to 11 530 Å). All measurements were made at 4.2 K. Measurements of the critical current with respect to the angle between the surface of the film and the magnetic-field direction revealed that a sharp critical current maximum occurs when the magnetic field is parallel to the film surface. For films thicker than 88.0 nm a broad maximum in the critical current was also observed when the orientation of the magnetic field was nearly perpendicular to the film. Films with a thickness between 25.0 and 60.0 nm carried the highest current densities in large magnetic fields. The ratio of the parallel critical magnetic field to the perpendicular critical magnetic field was less than 1.69 for films where the thickness was much greater than the coherence length. When the thickness was on the order of the coherence length the ratio was greater than 1.69 at 4.2 K.

17. Key Words (Suggested by Author(s))		18. Distribution Statement
Niobium	Critical current	Unclassified - unlimited
Superconductivity	Critical magnetic field	
Thin film		

19. Security Classif. (of this report)	20. Security Classif. (of this page)	21. No. of Pages	22. Price*
Unclassified	Unclassified	25	$3.00

*For sale by the National Technical Information Service, Springfield, Virginia 22151

SUPERCONDUCTING PROPERTIES OF NIOBIUM FILMS

by Wayne R. Hudson and Russell J. Jirberg

Lewis Research Center

SUMMARY

Critical currents as a function of magnetic field, film thickness, and film orientation have been studied for 14 niobium films ranging in thickness from 16.2 to 1153 nanometers (16.2 to 11 530 Å). All measurements were made at 4.2 K.

Measurements of the critical current with respect to the angle between the surface of the film and the magnetic-field direction revealed that a sharp critical current maximum occurs when the magnetic field is parallel to the film surface. For films thicker than 88.0 nanometers a broad maximum in the critical current was also observed when the orientation of the magnetic field was nearly perpendicular to the film. Films with a thickness between 25.0 and 60.0 nanometers carried the highest current densities in large magnetic fields.

The ratio of the parallel critical magnetic field to the perpendicular critical magnetic field was less than 1.69 for films where the thickness was much greater than the coherence length. When the thickness was on the order of the coherence length the ratio was greater than 1.69 at 4.2 K.

INTRODUCTION

Superconducting films are interesting because they have many practical applications and because their properties can provide information pertinent to the basic understanding of superconductivity. Some of the many practical applications (ref. 1) are current switches, modulators, amplifiers, transmission lines, microwave switching devices, and cryotron storage circuits. Most of these devices require qualitative and quantitative knowledge of the functional relations between critical current density, critical magnetic field, and film thickness.

Several papers have been published on the techniques of preparing superconducting niobium films (refs. 2 to 11). It was our intent to make an extensive study of the critical current density with respect to film thickness to determine whether some optimum

thickness exists. We also wanted to determine the variation of critical current with respect to the orientation of the films in a magnetic field. We have measured the critical current density of 14 films, ranging in thickness from 16.2 to 1153.0 nanometers (162 to 11 530 Å), with the magnetic field oriented both perpendicular and parallel to the plane defined by the film. The critical current I_c was also measured at specific values of magnetic-field strength while varying the angle between the field and the vector normal to the film surface from -30^o to 120^o. Niobium was chosen for this study because it is an inherently type II superconductor. It is more convenient to deposit niobium films and to study them than the alloys or intermetallic compounds of niobium. For the purpose of comparing with theory, the critical current densities of the films were calculated assuming that the current was concentrated primarily at the edges of the films.

Thin film superconductors are of fundamental interest because the surface effects can be studied independently of the bulk effects. Furthermore, when the film thickness d is on the order of the penetration depth λ or of the coherence distance ξ, there are interesting modifications of superconductivity. Both the penetration depth and the coherence distance are defined and discussed in reference 1. (Symbols are defined in appendix A.)

Another important phenomenon is surface superconductivity. When the magnetic field is parallel to the surface of a type II superconductor, the surface sheath exhibits a higher critical magnetic field than the bulk of the superconductor. This phenomenon is known as surface superconductivity. D. Saint-James and P. G. de Gennes (ref. 12) first predicted this result by solving the linearized Ginzberg-Landau equations. The analysis assumed that the half space $X > 0$ is occupied by metal and the half space $X < 0$ is either a vacuum or an insulator. These boundary conditions imply that ξ is much smaller than the bulk dimensions of the sample. Then, if the gage is chosen such that $A_x = A_z = 0$ and $A_y = HX$ and if the solution is assumed to be of the form $\psi = f(x)e^{iky}$, the equation takes the form of the Schrodinger equation for a harmonic oscillator. The lowest eigenvalue corresponds to the minimum of the potential being located a distance $X_o \approx 0.5901\ \xi(T)$ from the surface. Because the superconducting wave function is centered at the minimum of the potential and is concentrated in the region between X_o - (T) and X_o + (T), the solution implies that a surface superconducting state exists. A direct consequence of the solution is a relation between upper critical magnetic field H_{c2} and the critical field of the surface region H_{c3}. The theory predicts that $H_{c3} = 1.69\ H_{c2}$.

Thin films provide an interesting test of surface superconductivity, because for thick films $d/\xi >> 1$ and for thin films $d/\xi \approx 1$. Asada and Nose (ref. 13) have also studied surface superconductivity in niobium films. They found that $H_{c\parallel}/H_{c\perp} < 1.69$ for thick films $d/\xi >> 1$ and that $H_{c\parallel}/H_{c\perp}$ was greater than 1.69 when $d/\xi \approx 1$. We compare our results with the results of Asada and Nose and with the theory of surface superconductivity.

SAMPLES, APPARATUS, AND PROCEDURES

The 14 niobium films studied in the experiments described in this paper were prepared under contract by the National Bureau of Standards (ref. 14). All the films were vapor deposited onto Saphire substrates, which were held at 673 K. The deposition took place in a vacuum of 10^{-6} torr. Measurements of the critical temperatures T_c were provided with the films. The film thicknesses and critical temperatures are listed in table I. All the films are 0.318 centimeter wide.

The films were deposited in a dog bone geometry (fig. 1) in an attempt to minimize Joule heating at the current contacts. With the exception of two films (4 and 10) the films have an approximately rectangular cross-section. A sketch of the cross-section of films 4 and 10 is included in figure 1 This cross-section occurred accidently in film 4. It was probably caused by a slight shift in the deposition mask. Because of the large critical current density exhibited by film 4, a second film (film 10) was purposely deposited with this cross-section. Still another film was prepared specifically so that it could be examined with an electron microscope. This film was deposited on a copper plated substrate. Subsequently, it was floated free from the substrate with HNO_3. An electron microscope sample was prepared and figure 2 shows the photograph that was obtained. The photograph shows an extremely polycrystalline structure. The grain size ranges between 10.0 and 20.0 nanometers.

The thickness of each film was measured using an interference microscope. Two films of each thickness were deposited simultaneously. One film was used in the actual experiments, and the other was used to measure film thickness. The film used in the thickness measurements had a film of aluminum deposited over the top of the niobium.

The thickness of a niobium film was determined by measuring the wavelength of the destructive interference from fringes that result from a Fizeau interferometer. Figure 3 is a schematic of how the interference fringes are produced by the interferometer. A comparator plate, which has a partially silvered mirror on it, is placed on top of the film. Ninety-five percent of the light from a white-light source is reflected by the silver mirror and five percent is transmitted. The transmitted part is reflected by the aluminum film. When the thickness of the air layer between the comparator plate and the aluminum film is an integral number of half wave lengths, destructive interference occurs. When the reflected light is viewed with a spectroscope, a white light spectrum with interference fringes is observed (fig. 4). There is an abrupt change in the interference wavelengths, because the distance between the comparator plate and the aluminum film changes rapidly at the edge of the film. The longer wavelength corresponds to interference from the bottom of the step. The shorter wavelength corresponds to interference from the top of the step. Figure 4 is a photograph of the spectrum that was observed for film number 12. The thicknesses listed in table I are averages of five or more measurements. The thickness measurements are accurate to within 2.5 nanometers.

TABLE I. - NIOBIUM FILM PARAMETERS AND RESULTS

Film number	Thickness, nm	Critical temperature, K	Critical current peak at $\theta = 90^{o}$	$\theta_{1/2}$
1	16.2	6.9	No	3.8^{o}
7	25.6	6.86 - 8.9	No	9.5^{o}
2	29.2	7.9	No	0.5
3	40.9	8.7	No	1.8
10	16.8, 39.9 [a] 56.7	7.95	No	---
8	58.0	8.95	No	---
9	88.0	9.25	Yes	1
4	50.9, 41.2 [a] 92.1	8.9	No	0.8
11	176.7	8.75	Yes	1
5	227.7	9.3	Yes	1.5
12	298.0	9.3	Yes	1
13	799.0	9.45	Yes	2
13a	799.0	9.45	Yes	17
6	1153.0	9.3	Yes	0.5

[a]These two films were deposited such that they had a step at the edges. Both the total thickness and the thickness of the steps are tabulated.

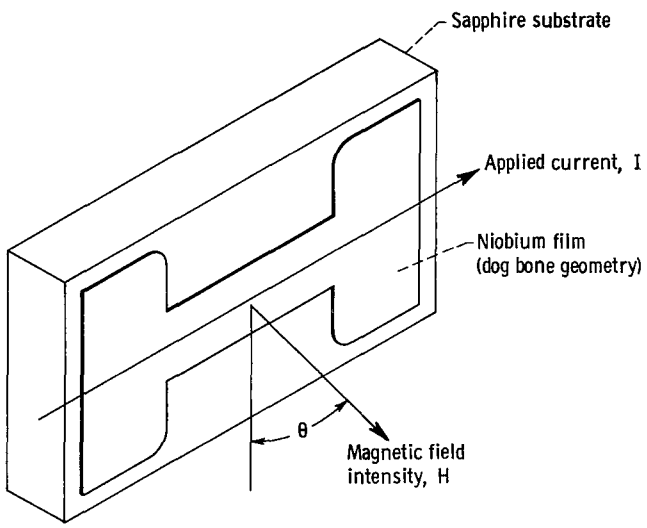

(a) Dog bone geometry of most films.

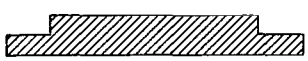

(b) Cross section of films 4 and 10.

Figure 1. - Experimental geometry and film cross-sectional area.

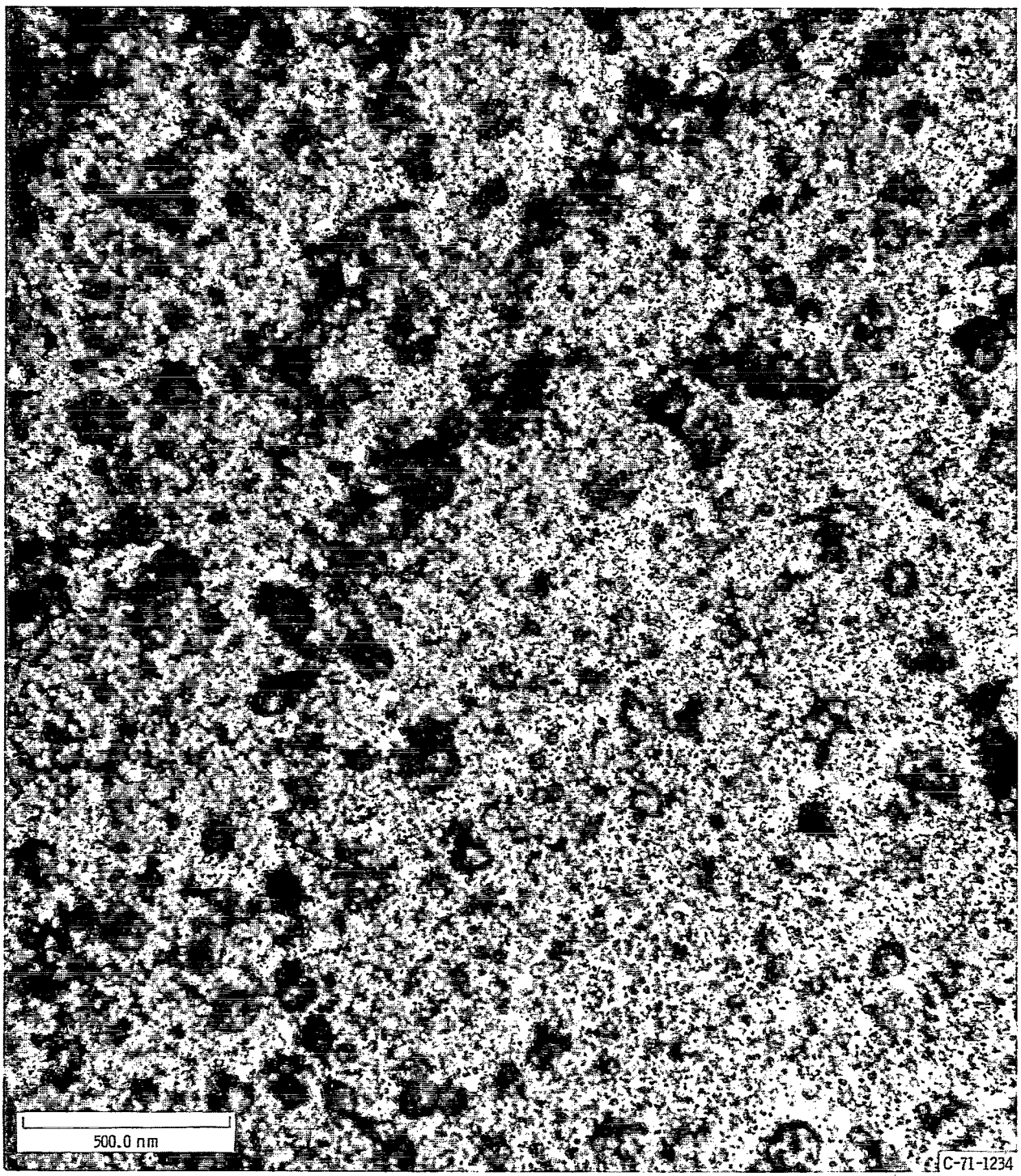

Figure 2. - Electron microscope picture of niobium film. Film was deposited on copper and then floated off in nitric acid. X72 000.

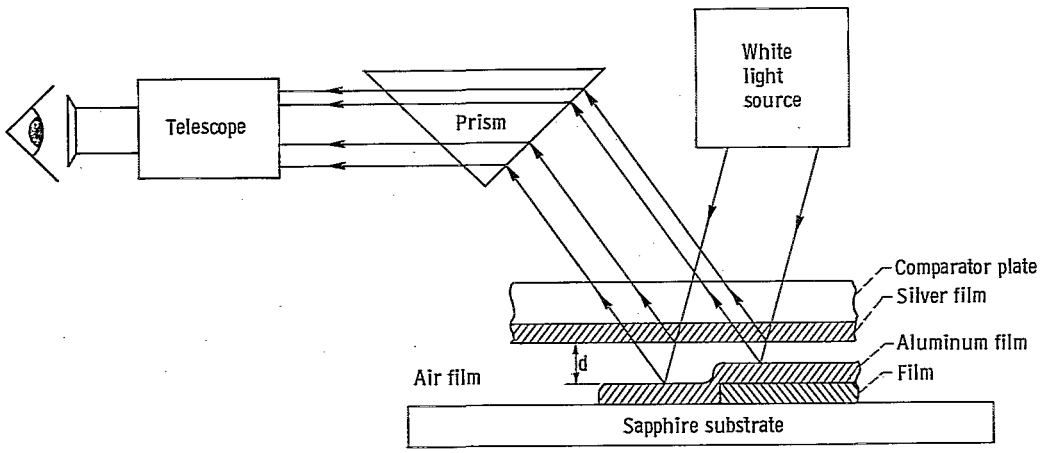

Figure 3. - Interference microscope and thickness measuring technique.

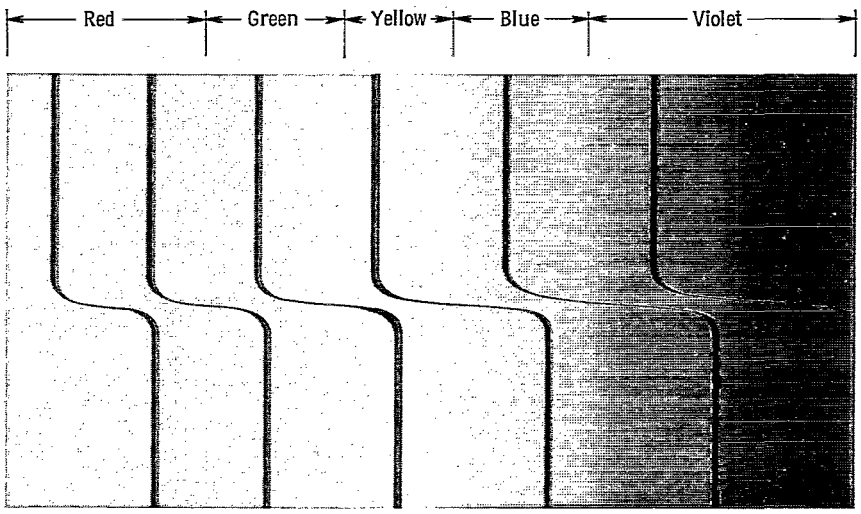

Figure 4. - White light spectrum with absorption-like lines as observed using interference microscope for film 12.

The apparatus used to measure critical currents consisted of a 1.5-tesla electromagnet with iron pole pieces, a liquid helium cryostat, a variable current supply, and a nanovoltmeter. The electromagnet was calibrated using nuclear magnetic resonance; in the experimental region the magnetic field was constant to one part in 10^4. The film was mounted in a sample holder (fig. 5), which was supported from the top of the cryostat. A scale on the support flange of the sample holder could be compared with a reference point on the top flange of the cryostat to determine the angular position of the film.

The critical current was measured as a function of magnetic field and the angle θ between the plane of the film and the magnetic field direction (fig. 1). The critical current was measured by slowly increasing the current through the sample until a voltage was observed across the sample. The voltage measuring sensitivity was 0.1 microvolt.

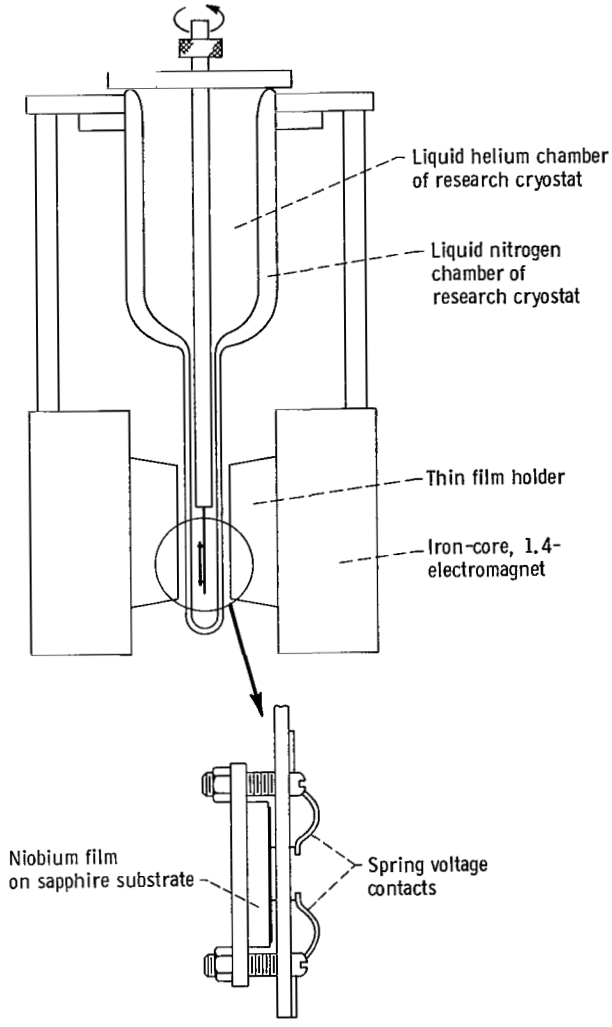

Figure 5. - Research apparatus, including electromagnet, research cryostat, and experimental probe.

Critical current measurements were made at fixed magnetic fields for various values of θ between 30° and 120°. The critical current was also measured with fixed values of 0° and 90°, varying the magnetic field over the range of the transition.

Because the electromagnet did not produce sufficient magnetic field to drive all of the films completely normal, it was necessary to repeat the critical-current-density versus field measurements for five of the films in a 5-tesla superconducting solenoid. In the superconducting solenoid, the angular orientations are only approximate. However, comparisons between data taken in both magnets indicate that the angular misalinement was probably less than 1°. Because Joule heating at the current contacts can be a major experimental problem, a carbon resistance thermometer was mounted on one contact. The

contact temperature was monitored during all critical current measurements. This procedure allowed us to discriminate between temperature transitions due to contact heating and transitions due to exceeding the critical current. For the samples tested the contact resistances were such that the onset of measurable contact heating occurred for current densities between 1×10^{10} and 1×10^{11} amperes per square meter.

RESULTS AND DISCUSSION

The experimental results fall naturally into three areas: the dependence of critical current on magnetic field orientation, the critical current density versus magnetic field intensity, and the ratio of $H_{c\parallel}$ to $H_{c\perp}$. In the discussion that follows the experimental results are discussed under these three areas in the order given.

Critical Current Dependence On Magnetic Field Orientation

All 14 films exhibited a sharp maximum in critical current when the magnetic field was parallel to the surface of the film ($\theta = 0^{o}$). A critical current maximum near $\theta = 90^{o}$ was also observed in six of the films tested.

Comparisons between individual films are complicated by the combination of the critical current-magnetic field characteristic for the thin films and the value of magnetic field at which the orientation data were measured. For example, figure 6 shows a comparison of critical current density as a function of magnetic field for the parallel and perpendicular orientations of film 2. The critical current density in the parallel orientation is greater at all values of magnetic field. In the perpendicular orientation the critical current density drops off sharply between 0.6 and 1.4 tesla. Above 1.4 tesla it becomes

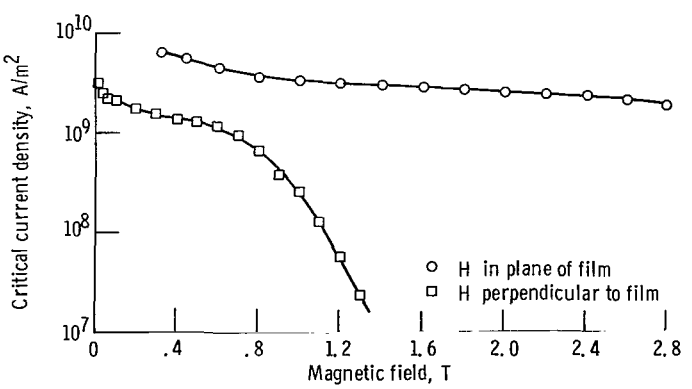

Figure 6. - Comparison between field parallel and field perpendicular critical current densities of film 2.

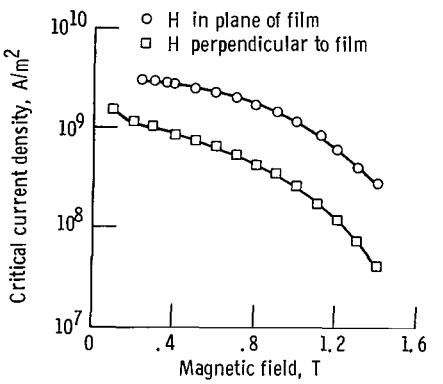

Figure 7. - Comparison between field parallel and field perpendicular critical current densities of film 6.

unmeasurably small. In contrast the critical current in the parallel orientation decreases only slightly up to 2.8 tesla. Clearly the dependence of critical current on orientation will depend strongly on the value of magnetic field. In the thicker films this effect is lessened as indicated by the critical current density versus magnetic field results obtained for film number 6 (fig. 7). Here the field-parallel critical current remains higher than the field-perpendicular critical current but never by more than a power of 10 in the region studied.

The dependence of critical current on magnetic field orientation is shown in figure 8 for the 14 different film thicknesses. The critical current maxima shown in figure 8 varied considerably in sharpness. As a rough measure of comparison between the films the angle at which the critical current had decreased to one half the maximum value, $\theta_{1/2}$, was used. The $\theta_{1/2}$ values are listed in table I. With the exception of films 1, 7, and 13a, the $\theta_{1/2}$ values are less than 2°. Several facts suggest that the broadening in the critical current maximum may be caused by impurities adsorbed onto or diffused into the films. The low critical temperatures of films number 1 and 7 (table I) is characteristic of films that have adsorbed gaseous impurities. Film 13a was purposely contaminated by the deposition of aluminum on it for making thickness measurements.

The critical current peaks centered at $\theta = 0^{\circ}$ are a direct result of surface superconductivity (ref. 12). As de Gennes and Saint-James have shown, in a decreasing magnetic field parallel to the surface of a superconductor, superconductivity first occurs at a field $H_{c3} = 1.69\ H_{c2}$. Between H_{c2} and H_{c3} a superconducting state exists, which is confined to a region within a few coherence distances of the sample surface. Therefore, when the applied magnetic field is parallel to the surface and of magnitude less than H_{c3}, there exists a surface layer of superconducting electrons. These superconducting electrons are available to carry currents and result in sharp critical current maximum near $\theta = 0^{\circ}$. The sharpness of the critical current maximum suggests that this effect might be useful as a magnetic field direction detector.

A critical current maximum was also observed near $\theta = 90^{\circ}$ in films 5, 6, 9, 11, 12, 13, and 13a. In each case the maximum at $\theta = 90^{\circ}$ was broader and of smaller magnitude than the maximum in the same film at $\theta = 0^{\circ}$. The $\theta = 90^{\circ}$ maximum was observed only in films 88.0 nanometers or thicker. One film (number 4) was thicker than 88.0 nm, but it did not exhibit a clear maximum at $\theta = 90^{\circ}$. As noted earlier film 4 was one of two films where the deposition mask was moved during its deposition. As a result, film 4 is not of uniform thickness. The edges are considerably thinner than the center region of the film (table I). Because the largest current in a thin film flows at the edges of the film and determines the film's critical current, film 4 exhibits the characteristics of a 40.0- or 50.0-nanometer film rather than a 92.0-nanometer film.

The critical current maximums centered near $\theta = 90^{\circ}$ have not been observed previously. To explain them we hypothesize that surface superconductivity can exist on the

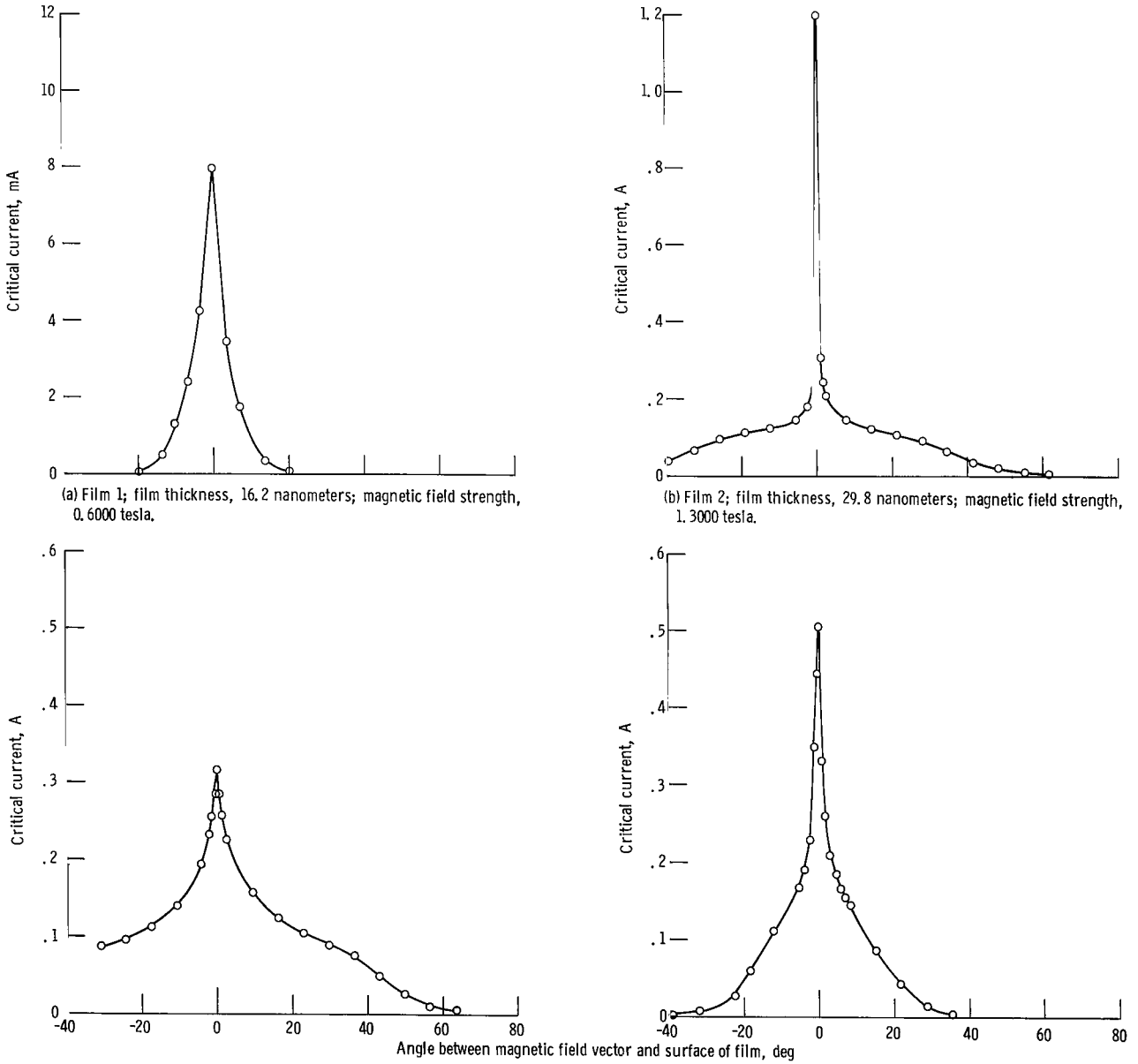

(a) Film 1; film thickness, 16.2 nanometers; magnetic field strength, 0.6000 tesla.

(b) Film 2; film thickness, 29.8 nanometers; magnetic field strength, 1.3000 tesla.

(c) Film 7; film thickness, 25.6 nanometers; magnetic field strength, 0.9000 tesla.

(d) Film 3; film thickness, 40.9 nanometers; magnetic field strength, 0.8500 tesla.

Figure 8. - Critical current of niobium films as function of angle between magnetic field vector and surface of film. Temperature, 4.2 K.

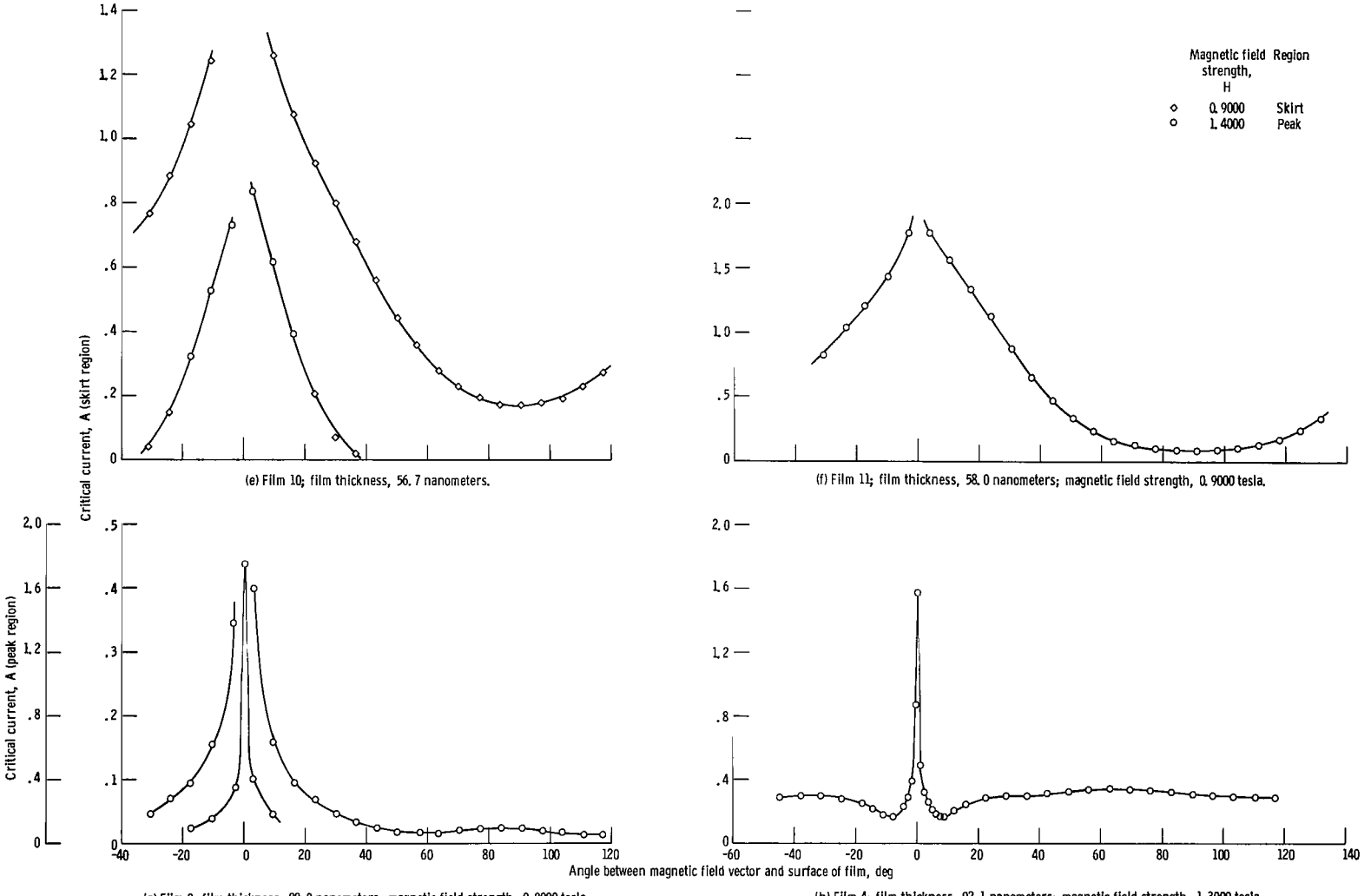

(e) Film 10; film thickness, 56.7 nanometers.

(f) Film 11; film thickness, 58.0 nanometers; magnetic field strength, 0.9000 tesla.

(g) Film 9; film thickness, 88.0 nanometers; magnetic field strength, 0.9000 tesla.

(h) Film 4; film thickness, 92.1 nanometers; magnetic field strength, 1.3000 tesla.

Figure 8. - Continued.

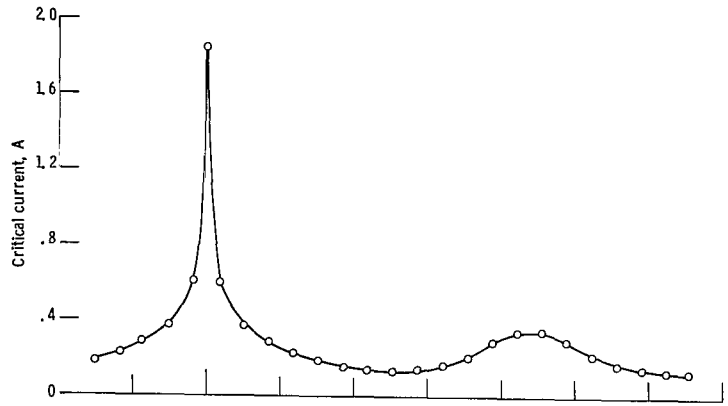

(i) Film 11; film thickness, 176.7 nanometers; magnetic field strength, 0.7000 tesla.

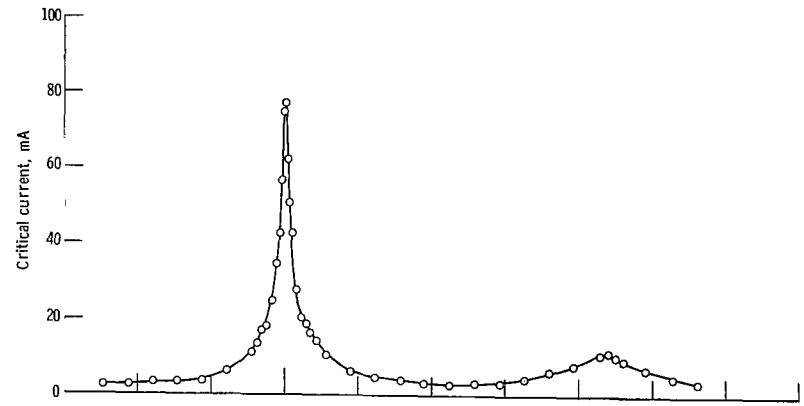

(j) Film 5; film thickness, 227.7 nanometers; magnetic field strength, 0.8500 tesla.

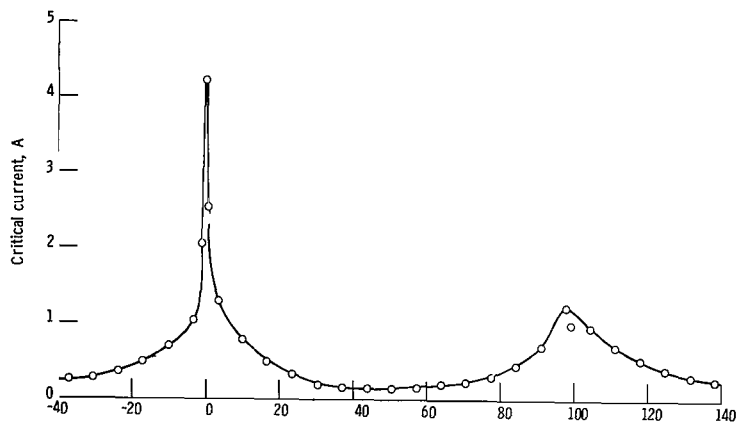

(k) Film 12; film thickness, 298.0 nanometers; magnetic field strength, 0.6000 tesla.

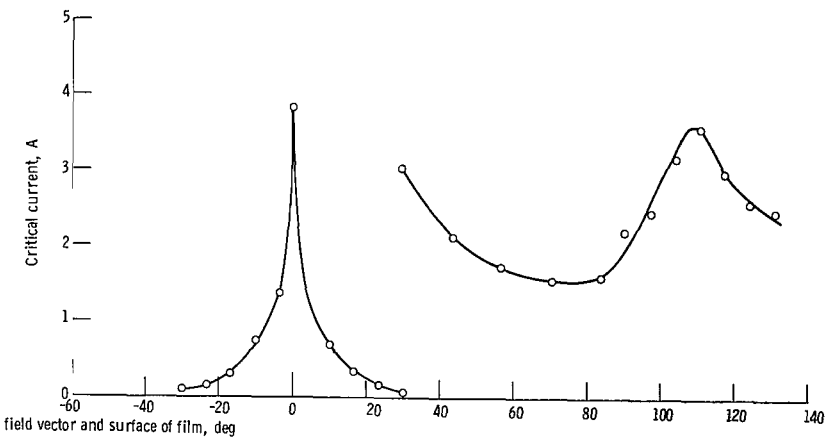

(l) Film 13; film thickness, 799.0 nanometers; magnetic field strength, 0.4000 tesla.

Figure 8. - Continued.

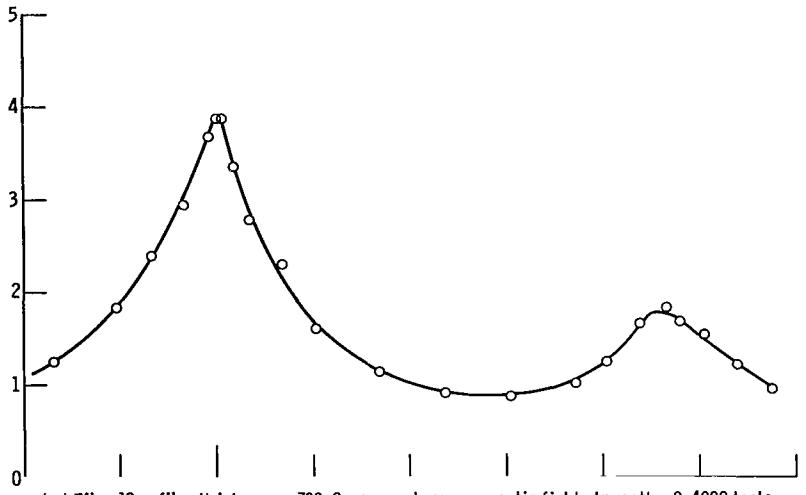

(m) Film 13a; film thickness, 799.0 nanometers; magnetic field strength, 0.4000 tesla.

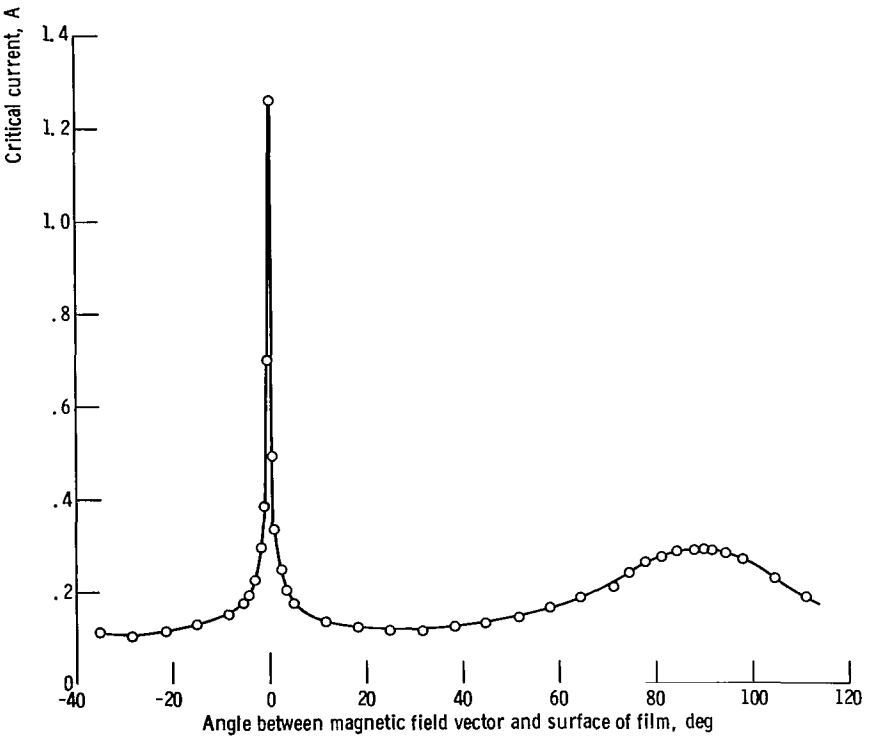

(n) Film 6; film thickness, 1153 nanometers; magnetic field strength, 1.3000 teslas.

Figure 8. - Concluded.

edge surfaces of the film when the film thickness is greater than a minimum value. In the derivation of the theory of surface superconductivity, it is assumed that the surface is infinite in extent. Experimental samples, of course, have surfaces of finite extent. To the best of our knowledge there is no established criterion for how narrow a superconducting surface can be and still exhibit surface superconductivity. The surface width would certainly have to be several times larger than the coherence distance. In the films investigated in this experiment the coherence distance is limited by the niobium grain size to about 15.0 nanometers. The thinnest film that exhibited a maximum at $\theta = 90^{o}$ was 88.0 nanometers thick or almost six times the coherence length.

Critical Current Density Dependence on Magnetic Field Strength

The measurements of critical current density versus magnetic field parallel to the film surface are shown in figure 9. It is obvious from the figure that there is a wide variation in the behavior between films. For the purposes of discussion the curves were divided into two groups. The first group (fig. 9(a)) which contains films 2, 3, 4, 7, 8, and 10 carried high current densities at relatively high magnetic fields (above 1.2 T). Films number 10 and 4 both had steps in their thicknesses as previously mentioned in the SAMPLES, APPARATUS, AND PROCEDURES section. If the current flows mainly near the edges of the film as suggested by the results of Glover and Coffey (ref. 15), then in films 10 and 4 the highest current would flow in the much thinner edges of the film (table I). The second group (fig. 9(b)) of films includes those whose current densities dropped off sharply below 1.2 teslas. Included in this group are films 6, 5, 9, 11, 12, and 13. These films are all 88.0 nanometers or thicker. In this group, the thicker the film, the lower the magnetic field where the current density drops off sharply.

The two general types of critical current density behavior may best be explained in terms of varying amounts of cold work. The characteristic shapes of the two groups of curves are very similar to curves discussed by Newhouse (ref. 1) for severely cold worked superconductors and annealed superconductors. It is reasonable to expect the thinner films to have more severe mechanical deformation. The first atomic layers of the deposit tend to replicate the structure of the substrate. Any imperfections in the substrate surface will also cause strains in films.

Film 1 was not included in either of the two groups, because the critical current density was too low to be put in group one and the critical current density did not fall off as sharply as the group two films did. The current density in film 1 is probably a result of its extreme thinness. When the film thickness is about equal to the grain size, the film will cease to behave like a planar film. Instead an ultra thin film has the properties of a "weakly connected" collection of grains. Such behavior might explain the low critical current density of film 1 (fig. 9(b)).

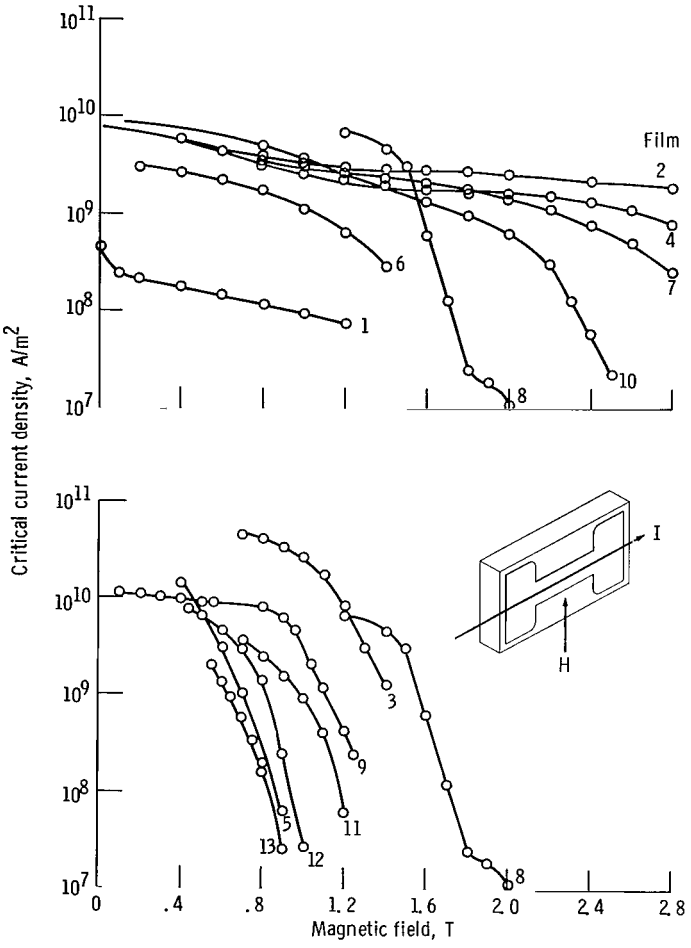

Figure 9. - Critical current density as function of magnetic field intensity in plan of film.

A comparison between the measured critical current density and the theoretically predicted value is hindered by the fact that the current is not distributed uniformly in planar films. The current density is largest at the edges of the film, and it is at the edges that the film first goes normal.

The current distribution will be assumed to be

$$J(x) = \frac{J(0)}{\left[1 - \left(\frac{2x}{w}\right)^2\right]^{1/2}} \tag{1}$$

where the film width is w, the distance from the center of the film is x, and $J(x)$ is the current density at x. This expression has been proposed by both Bowers (discussed in

ref. 15) and by Edwards (appendix 35.2 of ref. 1). The relation assumes that the current density is constant across the film thickness. This relation is in agreement with the experimental results of Rhoderick and Wilson (ref. 16). If it is integrated across the width of the film, the total current can be related to the current density at the center of the film,

$$I = 2\int_0^{w/2} \frac{d\,J(0)}{\left[1 - \left(\frac{2x}{w}\right)^2\right]^{1/2}} dx = wd\,J(0)\,\frac{\pi}{2} \tag{2}$$

where d is the film thicnesss. At the extreme edges of a flat rectangular film that obeys the London equations, Bowers found that

$$J(x) = J\left(\frac{w}{2}\right)e^{\left[-\left(\frac{1}{2}w-x\right)\frac{d}{\lambda^2}\right]} \tag{3}$$

Then by matching equation (1) and equation (3) where the slopes and magnitude are equal (ref. 15) the following expression is obtained:

$$J\left(\frac{w}{2}\right) = \left(\frac{ewd}{2}\right)^{1/2}\frac{J(0)}{\lambda} \tag{4}$$

where e is the base of the natural logarithms. Solving equation (2) for J(0) and substituting into equation (4) yield

$$J\left(\frac{w}{2}\right) = (2ewd)^{1/2}\,\frac{\bar{J}}{\pi\lambda} \tag{5}$$

where $\bar{J}$ is obtained by averaging the total current over the film cross-sectional area, $\bar{J} = I/wd$.

Equation (5) may be used to estimate the critical current density at the edges of the film. The value of $\bar{J}$ is measured, w and d are known, and λ can be estimated as described in appendix B. The largest $\bar{J}$ observed was 3.85×10^{10} amperes per square meter in film 3 at 0.8 tesla. Substituting this value of $\bar{J}$ along with $w = 0.318\times10^{-2}$ meter, $d = 4.09\times10^{-8}$ meter, and $\lambda = 4.3\times10^{-8}$ meter yields $J_c\left(\frac{w}{2}\right) = 7.5\times10^{12}$ amperes

per square meter. At 0.2 tesla most of the other films had average critical current densities, $\bar{J}_c$ between 3×10^9 and 1×10^{10} amperes per square meter. Using equation (5) again, the edge current densities fall between 1.0×10^{12} and 7.5×10^{12} amperes per square meter.

Theoretical estimates of the critical current density can be made for comparison. The critical current can be calculated assuming that the free energy between the normal and superconducting states is equal to the kinetic energy associated with the critical current. The resulting expression is

$$J_c = \frac{H_c}{\lambda_L} \tag{6}$$

Substituting the thermodynamical critical field of niobium determined by Finnemore, Stromberg, and Swenson (ref. 17) and $\lambda_L = 26.1$ nanometers from appendix B yields $J_c = 4.88\times10^{12}$ amperes per square meter. The agreement between the measured and calculated values is well within the accuracy of the measurements and calculations.

The Ratio of H_{c3} to H_{c2}

In the final part of this report the critical magnetic field H_{c2} and H_{c3} are estimated and compared with our experimental results for $H_{c\parallel}$ and $H_{c\perp}$ and the results of Asada and Nose (ref. 13).

The critical fields H_{c2} and H_{c3} are calculated in appendix A from estimates of the coherence distance, the penetration depth, and the mean free path. If the grain size limits the mean free path, then for $\lambda_{L0} = \xi_0 = 25.0$ nanometers and a grain size of 15.0 nanometers, the Ginzburg-Landau κ was calculated to be 4.10. Then from this estimate of κ and the definitions of H_{c2}, H_{c3}, and H_c from reference 17, the critical fields were determined to be 0.928 and 1.57 tesla, respectively.

For thick films ($d \gg \xi$), Tomasch and Joseph (ref. 18), and Burger, Deutscher, Guyon, and Martinet (ref. 19) showed that $H_{c\perp} = H_{c2}$ and that $H_{c\parallel} = H_{c3}$. They also found good agreement with the ratio of H_{c3} to H_{c2} predicted by de Gennes and Saint-James (ref. 12). For films where $d < \xi$ Saint-James (ref. 20) later pointed out that $H_{c\parallel}/H_{c\perp}$ can be much larger than 1.69.

Asada and Nose (ref. 13) have measured $H_{c\perp}$ and $H_{c\parallel}$ in niobium films where $d/\xi \approx 1$. They found that $H_{c\parallel}/H_{c\perp} \cong 5$ for a 20.0 nanometer film at $T/T_c = 0.9$, but at $T/T_c = 0.7$ they found $H_{c\parallel}/H_{c\perp} = 1.4$. The large value of the critical field ratio results from a sharp increase in $H_{c\parallel}$ for thin films. For a 29.2-nanometer film with $d/\xi = 1.9$, we measured and $H_{c\parallel}/H_{c\perp}$ of 3.6 at 4.2 K ($T/T_c = 0.53$). Asada and Nose also found

that in the thicker films they studied that $H_{c\parallel}/H_{c\perp} < 1.69$. In some of the films at $T/T_c = 0.7$ they found $H_{c\parallel} < H_{c\perp}$. At 4.2 K we did not find $H_{c\parallel}$ to be less than $H_{c\perp}$ for any of the films we investigated. But we did find examples of $H_{c\parallel}/H_{c\perp} < 1.69$. For films of d = 88.0 and 227.7 nanometers, $H_{c\parallel}/H_{c\perp}$ was measured to be 1.32 and 1.2, respectively.

CONCLUDING REMARKS

Measurements of the variation of critical current with the angle between the surface of the film and the direction of the magnetic field confirmed that a sharp critical current maximum occurs when the magnetic field is parallel to the film surface. For films thicker than 88.0 nanometers a broad maximum in the critical current was also observed when the magnetic field was nearly perpendicular to the film. The maximum in the parallel orientation is a result of surface superconductivity. This effect could be useful as a magnetic field direction detector. The perpendicular maximum has not been observed previously and is not understood.

The critical current-density - magnetic-field intensity characteristics of the films tested can be classified into two groups. One group consisting of films with thickness between 25.0 and 60.0 nanometers was capable of carrying high current densities in large magnetic fields. In one case at 4.08 tesla a 29.2-nanometer film had a critical current density of 0.75×10^5 amperes per square centimeter. The other group consisted of films that were not able to carry large current densities at high fields. All the films thicker than 100.0 nanometers fell into this second group. For applications requiring large current densities at high magnetic fields, films of about 30.0-nanometer thickness seem to be indicated. If the magnitude of the critical current densities is adjusted for the current distribution in the film, the critical current densities are within an order of magnitude of the predicted value.

The ratio of the parallel critical magnetic field to the perpendicular critical magnetic field was found to be less than 1.69 for films where the thickness was much greater than the coherence length. When the thickness was on the order of the coherence length the ratio was greater than 1.69 at 4.2 K. These results are similar to the results of Asada and Nose.

Lewis Research Center,
National Aeronautics and Space Administration,
Cleveland, Ohio, March 24, 1971,
129-02.

APPENDIX A

SYMBOLS

$\overline{A}$	magnetic vector potential
d	film thickness
e	base of the natural logarithms
f(x)	function of x
H	magnetic field strength
H_c	thermodynamic critical field (defined such that $H_c^2/8\pi$ is the condensation energy)
H_{c1}	magnetic field strength at which magnetic field first enters a superconductor
H_{c2}	magnetic field strength at which the magnetization of a superconductor equals zero
H_{c3}	magnetic field strength at which the state of surface superconductivity occurs
$H_{c\parallel}$	magnetic field strength parallel to the surface of a film that causes it to become resistive
$H_{c\perp}$	magnetic field strength perpendicular to the surface of a film that causes it to become resistive
I	total current
I_c	critical current, the current that is required to cause a superconductor to become resistive
i	imaginary unit, $\sqrt{-1}$
J(0)	current density at the center of the film
J(w/2)	current density at the film edge
J(x)	current density as a function of distance from the center of the film
$\overline{J}$	average current density (equal to the total current divided by the total cross-sectional area of the film)
$\overline{J}_c$	average critical current density
T	temperature in Kelvin
T_c	critical temperature

w	film width
X_0	value of the X coordinate where the harmonic oscillator potential is a minimum
X, Y, Z	rectilinear coordinates
κ	Ginzburg-Landau kappa
λ	penetration depth adjusted for nonlocal superconducting effects, $\lambda = \lambda_L \left(\frac{\xi}{\xi_0}\right)^{1/2}$
λ_L	London penetration depth
λ_{L0}	London penetration depth at absolute zero
ξ	coherence distance
ξ_0	coherence distance at absolute zero
θ	angle between the plane of the film and the magnetic field direction
$\theta_{1/2}$	value of theta at which the critical current is one-half the value at $\theta = 0$
ψ	quantum mechanical wave function

APPENDIX B

ESTIMATES OF ξ, λ, κ, H_{CZ}, AND H_{C3}

For the purpose of estimating the ξ, λ, κ, H_{c2}, and H_{c3} in niobium films, we assumed that $\lambda_{L0} = \xi_0 = 25.0$ nanometers and that a grain size of 15.0 nanometers, sets an upper limit on the electronic mean free path, Λ. Substituting these values into

$$\frac{1}{\xi} = \frac{1}{\xi_0} + \frac{1}{\Lambda}$$

yields

$$\xi = 9.35 \text{ nm}$$

The London penetration depth λ_L can be calculated for $T = 4.2$ K and $T = 9.3$ K from

$$\lambda_L(T) = \lambda_{L0}\left(1 - \left(\frac{T}{T_c}\right)^4\right)^{-1}$$

yielding

$$\lambda_L(4.2\text{K}) = 26.1 \text{ nm}$$

The nonlocal penetration depth is then

$$\lambda = \lambda_L(T)\left(\frac{\xi_0}{\xi}\right)^{1/2}$$

and

$$\lambda = 42.8 \text{ nm}$$

Then

$$\kappa \cong 0.96\,\frac{\lambda}{\xi} = 4.10$$

Next using $H_c(4.2K) = 0.160$ tesla from reference 17

$$H_{c2} = \sqrt{2}\,\kappa H_c = 0.928 \text{ tesla}$$

$$H_{c3} = 2.39\,\kappa H_c = 1.57 \text{ tesla}$$

REFERENCES

1. Newhouse, Vernon L.: Applied Superconductivity. John Wiley & Sons, Inc., 1964, ch. 6.

2. Fowler, Peter: Superconducting Niobium Films by Vacuum Deposition. J. Appl. Phys., vol. 34, no. 12, Dec. 1963, pp. 3538-3540.

3. Frerichs, R.; and Kircher, C. J.: Properties of Superconducting Niobium Films Made by Asymmetric ac Sputtering. J. Appl. Phys., vol. 34, no. 12, Dec. 1963, pp. 3541-3543

4. Theuerer, H. C.; and Hauser, J. J.: Getter Sputtering for the Preparation of Thin Films of Superconducting Elements and Compounds. J. Appl. Phys., vol. 35, no. 3, pt. 1, Mar. 1964, pp. 554-555.

5. London, H.; and Clarke, G. R.: Superconductivity of Thin Films of Niobium. Rev. Mod. Phys., vol. 36, no. 1, pt. 1, Jan. 1964, pp. 320-323.

6. Neugebauer, C. A.; and Ekvall, R. A.: Vapor-Deposited Superconductive Films of Nb, Ta, and V. J. Appl. Phys., vol. 35, no. 3, pt. 1, Mar. 1964, pp. 547-553.

7. Hauser, J. J.; and Theuerer, H. C.: Size Effects in Thin Films of V_3Ge, Nb, and Ta. Phys. Rev., vol. 134, no. 1A, Apr. 6, 1964, pp. 198-205.

8. Gerstenberg, D.; and Hall, P. M.: Superconducting Thin Films of Niobium, Tantalum, Tantalum Nitride, Tantalum Carbide, and Niobium Nitride. J. Electrochem. Soc., vol. 111, no. 8, Aug. 1964, pp. 936-942.

9. D'Yakov, I. G.; Lazarev, B. G.; Matsakova, A. A.; and Ovcharenko, O. N.: Critical Magnetic Fields of Superconducting Niobium Films. Soviet Phys.-JETP, vol. 19, no. 3, Sept. 1964, pp. 568-569.

10. Friebertshauser, P. E.; and Leder, L. B.: Superconducting Films of Niobium and Vanadium. Proceedings of the 14th National Vacuum Symposium, 1967, pp. 109-110.

11. Sosniak, J.; and Hull, G. W., Jr.: Superconductivity of Niobium Thin Films Deposited by dc Diode Sputtering. J. Appl. Phys., vol. 38, no. 11, Oct. 1967, pp. 4390-4392.

12. Saint-James, D.; and de Gennes, P. G.: Onset of Superconductivity in Decreasing Fields. Phys. Letters, vol. 7, no. 5, Dec. 15, 1963, pp. 306-308.

13. Asada, Yuji; and Nose, Hiroshi: Superconductivity of Niobium Films. J. Phys. Soc. Japan, vol. 26, no. 2, Feb. 1969, pp. 347-354.

14. Kamper, R. A.; Mullen, L. O.; and Sullivan, D. B.: Some Applications of the Josephson Effect. NASA CR-1565, 1970.

15. Glover, Rolfe E., III; and Coffey, Howard T.: Critical Currents of Thin Planar Films. Rev. Mod. Phys., vol. 36, no. 1, pt. 1, Jan. 1964.

16. Rhoderick, E. H.; and Wilson, E. M.: Current Distribution in Thin Superconductivity Films. Nature, vol. 194, no. 1167, June 23, 1962, pp. 1167-1168.

17. Finnemore, D. K.; Stromberg, T. F.; and Swenson, C. A.: Superconducting Properties of High-Purity Niobium. Phys. Rev., vol. 149, no. 1, Sept. 9, 1966, pp. 231-243.

18. Tomasch, W. J.; and Joseph, A. S.: Experimental Evidence for a New Superconducting Phase Nucleation in Type-II Superconductors. Phys. Rev. Letters, vol. 12, no. 6, Feb. 10, 1964, pp. 148-150.

19. Burger, J. P.; Deutscher, G.; Guyon, E.; and Martinet, A.: Angular Dependence of the Upper Critical Field of Type II Superconductors; Experiments. Phys. Letters, vol. 16, no. 3, June 1, 1965, pp. 220-221.

20. Saint-James, D.: Angular Dependence of the Upper Critical Field of Type II Superconductors; Theory. Phys. Letters, vol. 16, no. 3, June 1, 1965, pp. 218-220.

NASA-Langley, 1971 —— 26 E-6206

NATIONAL AERONAUTICS AND SPACE ADMINISTRATION
WASHINGTON, D.C. 20546

OFFICIAL BUSINESS
PENALTY FOR PRIVATE USE $300

FIRST CLASS MAIL

POSTAGE AND FEES PAID
NATIONAL AERONAUTICS AND
SPACE ADMINISTRATION

11U 001 51 51 3DS 71166 00903
AIR FORCE WEAPONS LABORATORY /WLOL/
KIRTLAND AFB, NEW MEXICO 87117

ATT E. LOU BOWMAN, CHIEF, TECH. LIBRARY

POSTMASTER: If Undeliverable (Section 158 Postal Manual) Do Not Return

"The aeronautical and space activities of the United States shall be conducted so as to contribute . . . to the expansion of human knowledge of phenomena in the atmosphere and space. The Administration shall provide for the widest practicable and appropriate dissemination of information concerning its activities and the results thereof."

— NATIONAL AERONAUTICS AND SPACE ACT OF 1958

NASA SCIENTIFIC AND TECHNICAL PUBLICATIONS

TECHNICAL REPORTS: Scientific and technical information considered important, complete, and a lasting contribution to existing knowledge.

TECHNICAL NOTES: Information less broad in scope but nevertheless of importance as a contribution to existing knowledge.

TECHNICAL MEMORANDUMS: Information receiving limited distribution because of preliminary data, security classification, or other reasons.

CONTRACTOR REPORTS: Scientific and technical information generated under a NASA contract or grant and considered an important contribution to existing knowledge.

TECHNICAL TRANSLATIONS: Information published in a foreign language considered to merit NASA distribution in English.

SPECIAL PUBLICATIONS: Information derived from or of value to NASA activities. Publications include conference proceedings, monographs, data compilations, handbooks, sourcebooks, and special bibliographies.

TECHNOLOGY UTILIZATION PUBLICATIONS: Information on technology used by NASA that may be of particular interest in commercial and other non-aerospace applications. Publications include Tech Briefs, Technology Utilization Reports and Technology Surveys.

Details on the availability of these publications may be obtained from:

SCIENTIFIC AND TECHNICAL INFORMATION OFFICE

NATIONAL AERONAUTICS AND SPACE ADMINISTRATION

Washington, D.C. 20546